Electrochemical Impedance Spectroscopy (EIS) and Study of Iron Corrosion Inhibition by Turmeric Roots Extract (TRE) in Hydrochloric Acid Solution

Kholod Almzarzie, Ahmad Falah*, Ayman Massri and Hassan Kellawi
Department of Chemistry, Faculty of Science, Damascus University, Syria.

TURMERIC Root extract (TRE) was tested as corrosion inhibitor for iron in 0.5 M HCl, using potentiodynamic polarization and electrochemical impedance spectroscopy (EIS). Scanning electron microscope (SEM), and energy dispersive X-rays (EDX) analysis. The inhibition efficiency raised as in time of immersion rises, but decreases with temperature rise. The Nyquist plots showed that, the charge transfer resistance (Rct) increase, and the double layer capacitance (C_{dl}) decreases with time of immersion increase. Tafel results exhibit that both corrosion current and with corrosion speed are reduced with time of immersion. All impedance spectra of EIS tests exhibit one capacitive loop which indicates that the corrosion reaction is controlled by charge transfer process. IE (%) increases with the concentration of the inhibitor reaching its maximum value, 88. 90%, at 8g/100ml. Thermodynamics parameters: Ea, ΔH*, ΔS* were estimated, and mechanism of corrosion and inhibition was discussed. The adsorption of (TRE) followed Langmuir adsorption isotherm.

Keywords: Iron, Electrochemical Impedance Spectroscopy (EIS), Turmeric Root extract (TRE), double layer capacitance (C_{dl}), Scanning electron microscope (SEM).

Introduction

Inhibition of corrosion of iron is demanding for theoretical and practical aspects [1]. Iron and its alloys are of great importance in the industry, prompting vast research on corrosion resistant and its conducts [2]. Acids are wildly used in industries [3], such as industrial acid cleaning, acid descaling, acid picking, and used to remove mill scale from metallic surfaces. Natural compounds containing sulphur, oxygen and nitrogen atoms are effective as corrosion inhibitors in acid media, Inhibitors are used to reduce the rate of dissolution of metals [4]. Organic compounds containing heteroatoms are commonly used to reduce the corrosion process of iron in acidic media [5]. The use of non-toxic inhibitors called green or ecofriendly environmental inhibitors is one of the solutions possible to prevent corrosion of molten [6]. The adsorption of these compounds is influenced by the Electronic structure of their content of active compounds, electrons density, aromatic rings, and functional groups possessing free electrons such as, R–OH –CHO, –N=N etc.., [7]. The adsorption of organic inhibitors at the metal/solution interface takes place through the replacement of water molecules by organic inhibitors molecules [8]. The efficiency of these compounds depends mainly on their abilities to be adsorbed on the metal surface with their polar groups moving as the reactive centers. The purpose of this research is to use a non-toxic environment-friendly inhibitor formed from Turmeric Root extract to reduce iron corrosion and study its effect using electrochemical Impedance and Tafel polarization methods.

Materials and Methods

Preparation of plant extract

The turmeric extract is prepared by washing, drying the turmeric root and grinding it then dissolving 1 g of powder in 100 ml methanol 50%, and removing the solvent by placing the solution in the vacuum evaporator, at 60°C. Distilled water is used in the preparation process [9].

Preparation of metal specimen

The iron specimens having composition (wt%) of 0.200% C, 0.500% Si, 1.600% Mn, 0.035% S, 0.035% P, 0.040Nb, 0.012N, 0.020Al, and remaining Fe were abraded with a series of emery papers 400,1200,1500, 2000 grades. The samples

were then washed thoroughly with distilled water, and dried with air.

Test Solution

A solution of 0.5M concentrated acid was prepared using distilled water and 37% hydrochloric acid.

Electrochemical Measurements

Electrochemical measurements were carried out using potentiostat IVIUM-STAT.XR (Holland) piloted by voltammetry software. A three electrodes cell system containing working electrode (iron coupon) of a 1 cm² exposed area, saturated $(Ag/AgCl_2)$ electrode as a reference electrode and a platinum wire as auxiliary electrode were used. The electrochemical impedance spectroscopy (EIS) measurements were carried out using the above electrochemical system, polarization curves were recorded at a sweep rate of 50 mV.s⁻¹, Electrochemical impedance spectroscopy (EIS) measurements were carried out at open-circuit potential over a frequency range of 1MHz - 1Hz. The sinusoidal perturbation was amplitude of 0.01mv.

Scanning electron microscopy (SEM), Energy dispersive X-rays (EDX)

Inhibitor film formation of the extracts surface was studied and compound using SEM and EDX Technique.

Results and Discussion

Mechanism of inhibition process Mechanism of inhibition process

The Turmeric Root extract (TRE) used here as a corrosion inhibitor can serve as a scale inhibitor as well. This plant is characterized by the percentage of phenolic compounds (Categories of curcumin) of a percentage up to 90%. It is natural - non-toxic - environmentally friendly material. Active compounds in Turmeric Root extract (TRE) are attributed to curcumin, demethoxy curcumin, bis demethoxy curcumin, and to the multiple lone pair of electrons, multiple bonds and/or conjugated Π-type bond system [10]. Adsorption of these active molecules forms thin inhibitor films on the metal surface which isolate the metal- surface from the corrosive environment [11]. The oxygen atoms -The aromatic rings-and the bilateral bond - of the aromatic rings boosts the electronic pair freedom on the surface of the electrode. These compounds adsorb their free electrons on the surface of the electrode, and the iron is oxidized to form positively charged iron, thus forming a double electrical layer and difference in voltage arises, as schematically presented in Fig. 1. The inhibitor enhances the free electrons, which reduces iron corrosion and enhances inhibition.
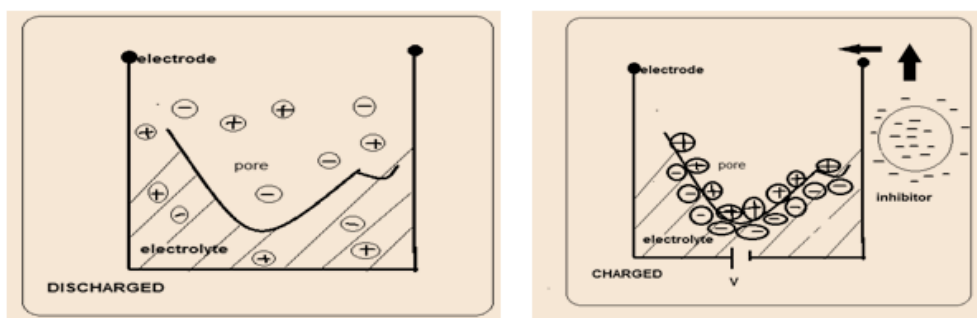

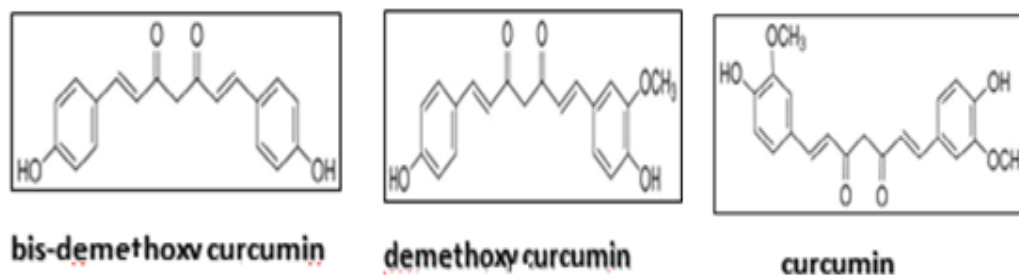**Fig. 1. Schematic presentation of the Electric Double –Layer formation.**

Fig. 2. Active compounds in Turmeric Root extract (TRE).

Electrochemical impedance spectroscopy measurements

The corrosion behavior of iron in 0.5M HCl solution, in the absence and presence of TRE, it investigated by the EIS, at 298 K after 1 hour of immersion in the acid solution. The double layer capacitance (C_{dl}) and the frequency at which the imaginary component of the impedance is maximum ($-Z_{max}$) are found via the equation:

$$C_{dl} = 1/w_{max}R_{ct} \qquad \text{where} \qquad w_{max} = 2\pi f_{max} \qquad (1)$$

The inhibition efficiency % IE_{Rct} resulted from the charge transfer resistance (R_{ct}) is calculated by:

$$\% \, IE_{Rct} = [(R_{ct} - R^0_{ct})/R_{ct}]_* 100 \qquad (2)$$

where R^0_{ct} and R_{ct} are the charge transfer resistance (R_{ct}) in the absence and presence of different concentrations of inhibitor, respectively [12].

Nyquist's and Bode's graphs of the results of the EIS of iron in 0.5M HCl, in absence and presence of different concentrations of TRE were presented in Fig. 3 and 4 respectively. The big capacitive loop refers to the adsorption of the inhibitor molecules (active compounds) presented in Fig. 2 on the iron samples [13]. The existence of single semi-circle indicated the single charge transfer process during dissolution which is unaffected by the presence of inhibitor molecules. Deviations of ideal circular shape are often referred to the frequency dispersion of interfacial impedance, which could be due to the roughness and other inhomogeneity of the surface, constant phase element (CPE) with the exponential factor (α) expressed about degree of roughness [14]. As seen in Table 1, the R_{ct} values of inhibited substrates increased with the concentration of inhibitors. Further, the values of C_{dl} decreased which perhaps was compounds extract due to the decrease in local dielectric constant and/or increase in thickness of the electrical double layer, which suggests that TRE acts via adsorption at the metal/solution interface [15]. Equivalent circuit model used to fit impedance spectra data present in Fig. 5.
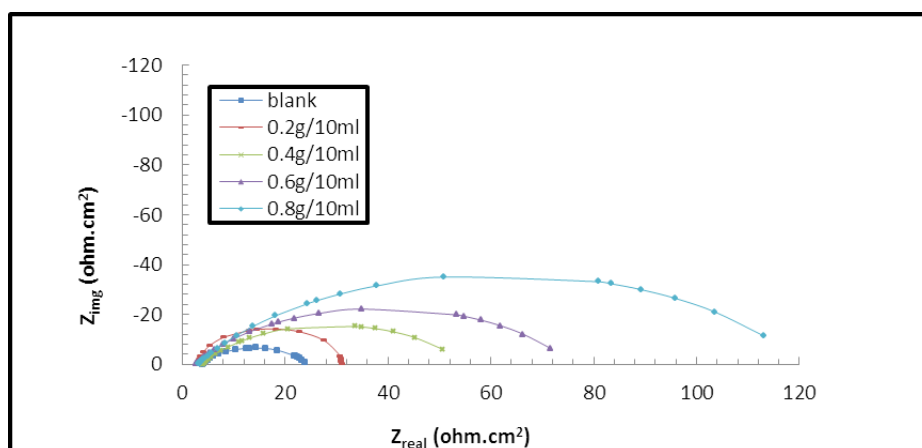

Fig. 3. Nyquist plots of iron in 0.5M HCl containing varying concentrations of TRE after 1hour of immersion in acid solution.
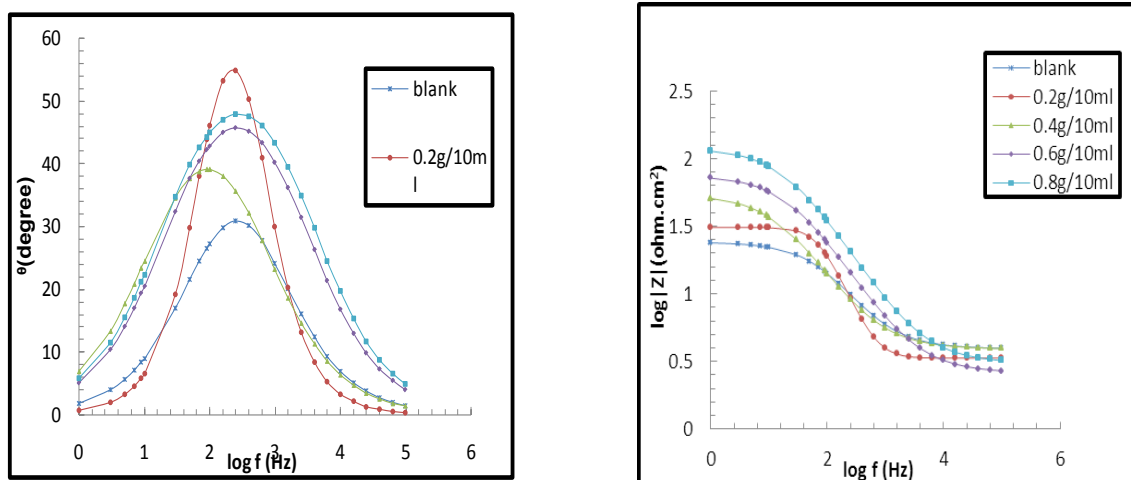

Fig. 4. Bode plots of iron in 0.5M HCl containing varying concentrations of TRE after 1hour of immersion in acid solution.
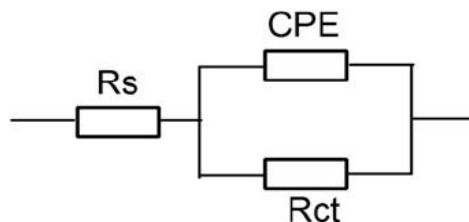
Fig. 5. Equivalent circuit model used to fit impedance spectra data.

TABLE 1. Impedance parameters of corrosion of iron in 0.5M HCl at 298K in the absence and presence of different concentrations of TRE.

Inhibitor	conc (g/100ml)	R_{ct} (ohm)	f_{max} (Hz)	C_{dl} (F/cm²)	α	IE_{Rct}%
Blank	0.0	20.3	160	$4.90*10^{-5}$	0.73	-------
Turmeric Root extract (TRE)	2.0	27.7	160	$3.59*10^{-5}$	0.98	26.71
	4.0	50.8	100	$3.13*10^{-5}$	0.70	60.04
	6.0	73.1	160	$1.36*10^{-5}$	0.70	72.23
	8.0	117	160	$8.51*10^{-6}$	0.70	82.65

Potentiodynamic polarization measurements
   Influence of concentration

Polarization measurements were done in order to know about the kinetics of the cathodic and anodic reactions. The anodic and cathodic current–potential curves are extrapolated up to their intersection at appoint where corrosion current density (I_{corr}) and corrosion potential (E_{corr}) are acquired [16]. Table 2 shows the electrochemical parameters (I_{corr}, E_{corr}, βa, βc, and CR) obtained from Tafel plots for the iron electrode in 0.5M HCl solution without and with various concentrations of TRE. The I_{corr} values were used to calculate the inhibition efficiency, IE (%), in Table 2, using the following equation:

$$IE = [I-I_{corr}/I]_*100 \tag{3}$$

where I_{corr} and I are the corrosion current densities with presence and absence of inhibitor, respectively. The CR values in Table 2, using the following equation [17]:

$$CR = 3.27*10^{-3} i_{corr} E_w/d \tag{4}$$

where i_{corr} is the corrosion current density in micro A/cm², E_w is the equivalent weight of the corroding metal in grams, and d is the density of the corroding metal in g/cm³.

Under the experimental conditions performed, the cathodic section of the plot represents the hydrogen evolution reaction, while the anodic section represents the iron dissolution reaction. They are determined by extrapolation of Tafel lines to the respective corrosion potentials.

TABLE 2. Electrochemical parameters of iron in 0.5M HCl solution at different concentrations without and with TRE.

Inhibitor	conc (g/100ml)	$-E_{corr}$ (mV/SCE)	I_{corr} (A*10⁻⁴/cm²)	βa (mV/dec)	βc (mV/dec)	CR (mm/y)	IE%
Blank	0.0	0.677	26.13	0.352	0.183	8.56	----
Turmeric Root extract (TRE)	2.0	0.3968	10.8	0.155	0.323	3.54	58.67
	4.0	0.474	4.7	0.146	0.233	1.55	82.01
	6.0	0.453	3.8	0.139	0.179	1.25	85.46
	8.0	0.417	3.4	0.131	0.225	1.11	86.99

The results in Table 2 indicates that the inhibitor reduces the corrosion current value and inhibition, IE (%) increases with the concentration of the inhibitor reaching its maximum value, 88. 90%, at 8g/100ml. This result suggests that the mechanism of the electrode reaction is not changed [18].

TABLE 3. Polarization parameters of iron in 0.5M HCl at different temperatures with various concentration of TRE.

T(K)	Conc (g/100ml)	$-E_{corr}$ (mV/SCE)	I_{corr} ($\mu A/cm^2$)	βa (mV/ dec)	βc (mV/ dec)	CR mm/y	IE%
283	Blank	0.677	26.13	0.352	0.183	8.56	-------
	2	0.3968	10.8	0.155	0.323	3.54	58.67
	4	0.468	5.9	0.148	0.177	1.933	77.42
	6	0.453	3.8	0.139	0.179	1.25	85.46
	8	0.442	2.9	0.143	0.188	0.979	88.90
293	Blank	0.661	31.1	0.316	0.174	10.19	-------
	2	0.379	8.35	0.142	0.328	2.73	73.15
	4	0.458	6.6	0.138	0.205	2.167	78.78
	6	0.458	4.8	0.164	0.206	1.581	84.57
	8	0.441	4	0.131	0.193	1.318	87.14
303	Blank	0.677	33.8	0.331	0.168	11.07	------
	2	0.452	13.5	0.167	0.249	4.4	60.06
	4	0.426	9	0.132	0.263	2.97	73.37
	6	0.474	7	0.152	0.193	2.29	79.29
	8	0.498	5.7	0.14	0.16	1.87	83.14
313	Blank	0.714	36.2	0.378	0.119	11.84	------
	2	0.477	14.6	0.188	0.237	4.788	59.67
	4	0.419	11	0.135	0.28	3.631	69.61
	6	0.379	7.9	0.133	0.339	2.6	78.18
	8	0.468	5.9	0.148	0.177	1.933	83.70

Influence of temperature

Polarization curves for the iron in 0.5 M HCl solution are shown in Fig. 6 and 7 in two different conditions, with constant concentrations of TRE and in the presence of different concentrations of TRE in the temperature range 283-313K.

The numerical values of the corrosion current density (I_{corr}), corrosion potential (E_{corr}), anodic Tafel slope (βa), cathodic Tafel slope (βc), and the degree of surface coverage (Θ) vis the concentrations of inhibitor (TRE) at various temperatures are given in Table 3. These values were calculated from the intersection of the cathodic and anodic Tafel lines of the polarisation curve at E_{corr}. The surface overage (Θ) was calculated using:

$$\Theta = IE (\%) /100 \quad (5)$$

The inhibition efficiency IE (%) is given by equation 3.

The results of Table 3 refer that temperature increase leads to I_{corr}, increase while the addition of TRE resulted in decrease of the I_{corr} values across the temperature range. The results also indicate that the inhibition efficiencies increased with the concentration of inhibitor but decreased proportionally with temperature. Such behavior can be rationalized that the inhibitor acts by adsorption onto the metal surface [19].
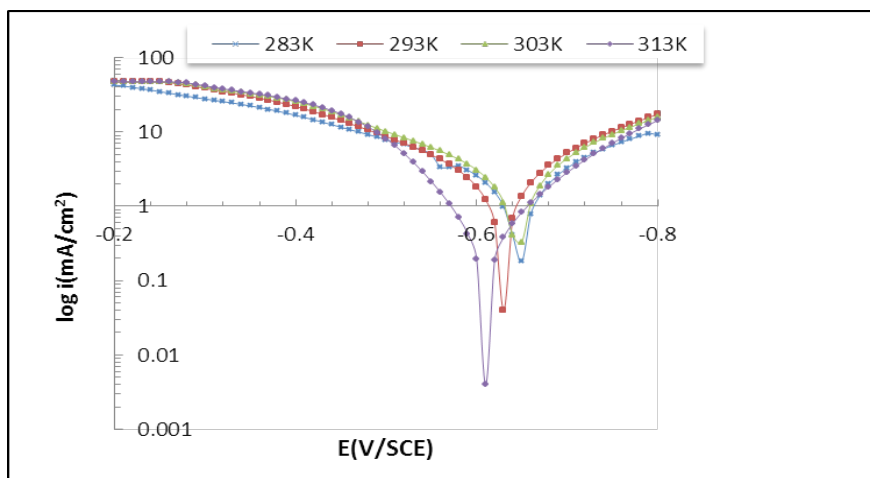
Fig. 6. polarization curves of iron in 0.5M HCl at different temperatures.
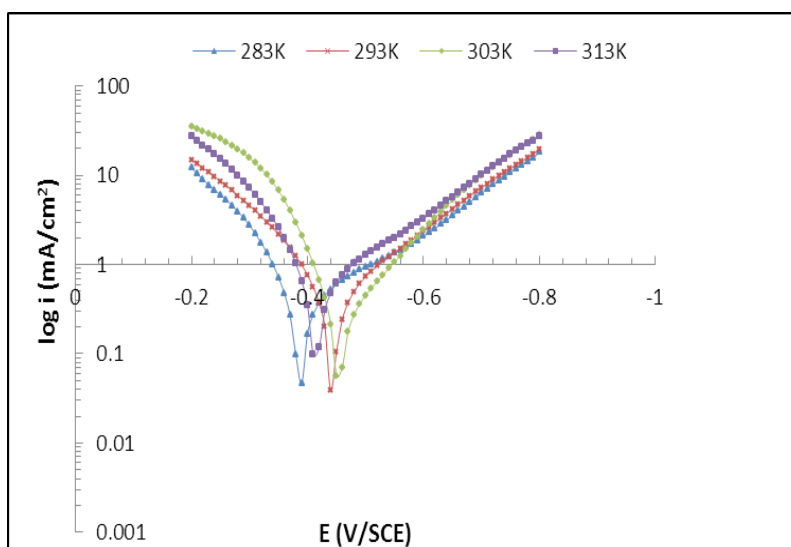
Fig. 7. polarization curves of iron in 0.5M HCl at different temperatures in the presence of 8g/100ml of TRE.

Activation parameters such as the activation energy, Ea, the entropy of activation, ΔS^*, and the enthalpy of activation, ΔH^*, for both corrosion inhibition and corrosion of iron in 0.5 M HCl in the presence and absence of TRE at different concentrations between 283 and 313K were calculated from an Arrhenius-type plot (Eq. 6) and transition state (Eq. 7) [20]:

$$\text{Log } (I_{corr}) = - E_a/2.303RT \qquad (6)$$

where I_{corr} is the corrosion current density (taken from averaged polarization), Ea is the activation energy, and R is the universal gas constant.

$$I = \frac{RT}{Nh} \exp\left(\frac{\Delta S*}{R}\right) \exp\left(-\frac{\Delta H*}{RT}\right) \qquad (7)$$

where h is Planck's constant, N is Avogadro's number, ΔH^*_a is the enthalpy of activation, and ΔS^*a is the entropy of activation.

Plots of Log (I_{corr}) vs. 1/T and Log (I_{corr}/T) vs. 1/T gave straight lines with slopes of -Ea/R and $-\Delta H^*$ /R, respectively. The intercepts were A and [Ln (R/Nh) + $(\Delta S^*$ /R)] for the Arrhenius and transition state equations, respectively. (Fig. 8 and 9). The calculated values of the activation energy Ea, the entrpy of activation ΔS^*, and the enthalpy of activation ΔH^* are presented in Table 4.
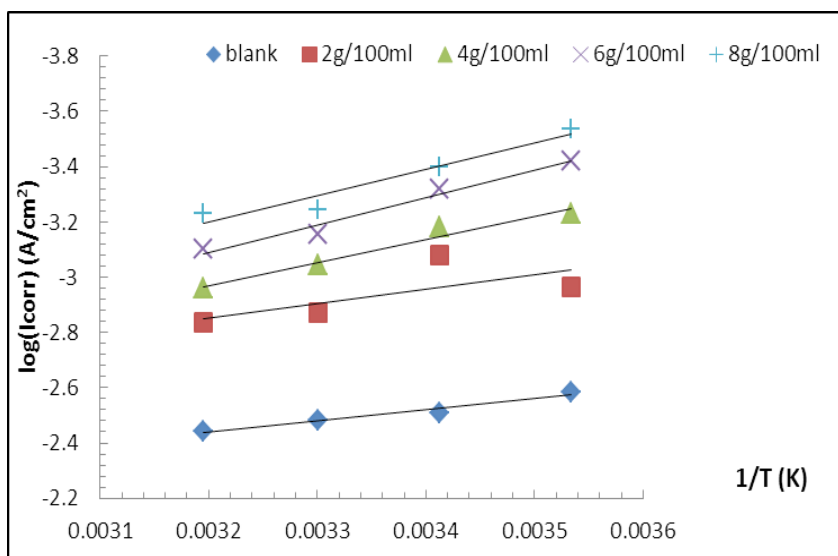

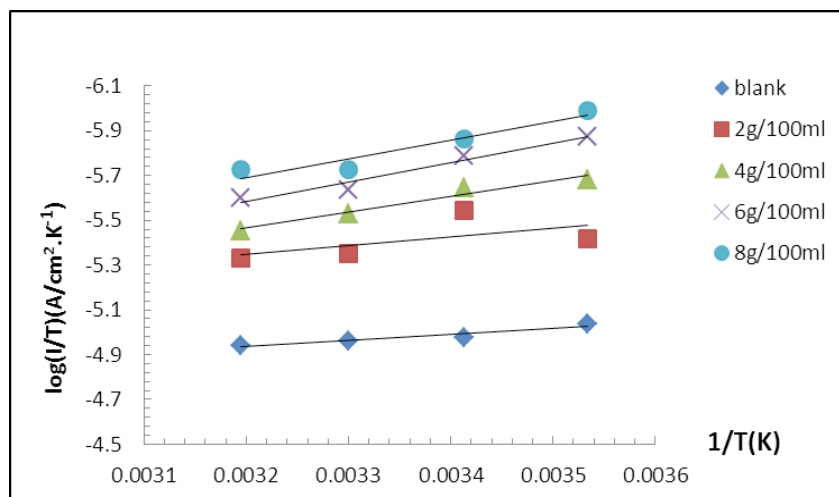**Fig. 8. Arrhenius plots of log $(I_{corr)}$ versus 1/T at various concentration of TRE.**

Fig. 9. variation of log (I$_{corr}$/T) versus 1/T at various concentrations of TRE.

The activation energy rises somewhat with increasing inhibitor concentration, suggesting adsorption of inhibitor molecules at the metal surface. The increase in the activation energy could be due to the corrosion reaction mechanism in which charge transfer was blocked by the adsorption of TRE molecules on the iron surface [21]. It also revealed that the whole process was controlled by the surface reaction since the energy of the activation corrosion process in presence of TRE was nearer to 20 kJ mol^{-1}.

As seen in Table 4, the values of ΔH* were approximate, and the values of Ea, increased for the corrosion of iron in the presence of inhibitor by up to 80%, indicating that the energy barrier for

the corrosion reaction increased in the presence of inhibitor without change of the dissolution mechanism [22]. The entropy of activation, ΔS*, was negative both in the absence and presence of inhibitor, implying that the activated complex represented the rate-determining step with respect to the association rather than the dissociation step. This implies that a decrease in disorder occurred when proceeding from statc of reactants to the activated complex [23].

In addition, the less negative values of ΔS* in the presence of inhibitor imply that the presence of inhibitor created a quasi-equilibrium corrosion system state.

TABLE 4. values of activation parameters ΔS* and ΔH* for iron 0.5MHCl in the presence and absence of various inhibition concentrations.

Inhibitor	C(g/100ml)	Ea(kJ/mol)	ΔH* (kJ/mol)	ΔS* (J/mol)
0.5M HCl	----	7.69	5.22	-275.37
Turmeric Root extract (TRE)	2.0	10.02	7.55	-275.83
	4.0	15.99	13.52	-258.93
	6.0	18.99	16.52	-251.65
	8.0	18.43	15.96	-255.51

Adsorption isotherm

Adsorption isotherm study describes the adsorptive behavior of organic inhibitors to understand the adsorption mechanism. The most usually applied adsorption isotherms are Frumkin, Temkin, and Langmuir. The surface coverage (Θ) values for the inhibitor concentration used were calculated using polarization measurements.

Langmuir adsorption isotherm was tested and found most appropriate isotherm to fit the

experimental data. Langmuir adsorption isotherm is represented by the following equations [24]:

$$\log (\Theta/1- \Theta) = \log K + Y \log C \qquad (8)$$

Rearrangement gives the following equation

$$C\backslash\theta = 1/K_{ads} + C \qquad (9)$$

Where, θ is the degree of surface cover with the inhibitor, Y is the slope; number of layers. K$_{ads}$ is the adsorption equilibrium constant and C is the

concentration of inhibitor used in the corrosive medium.

A straight line was obtained by plotting C/Ө vs C with the R^2 value almost unity (0.99) (Fig. 10).

The calculated slope is almost unity suggesting that the Langmuir adsorption isotherm model provides the best description of the adsorption behavior.
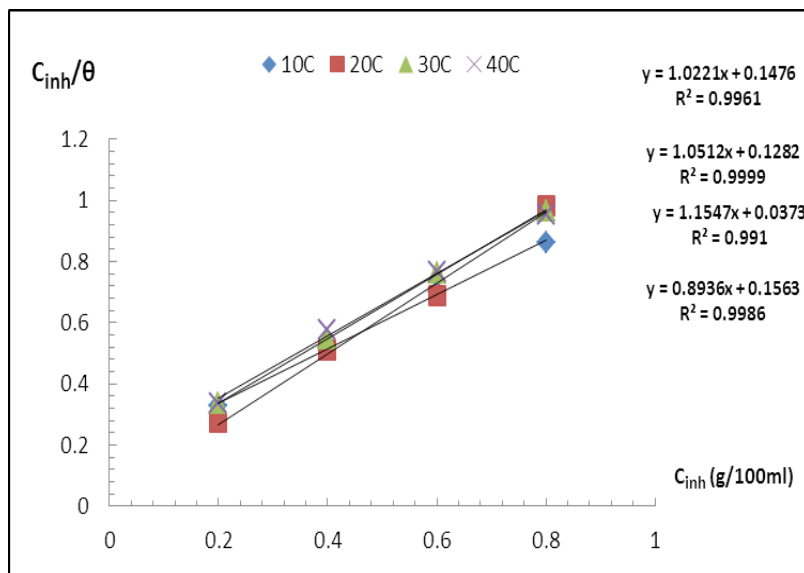

Fig. 10. Plots of Langmuir adsorption isotherm of TRE on iron surface at different temperatures.

TABLE 5. Calculated parameters of Langmuir adsorption isotherm.

T(K)	1/K	ΔGa (kJmol^{-1})	ΔSa (Jmol^{-1})	R^2	ΔHa(kJmol^{-1})
283	0.16	-13.8169	48.75	0.9986	
293	0.04	-17.7954	60.67	0.9910	-20
303	0.13	-15.2926	50.40	0.9999	
313	0.15	-15.4306	49.24	0.9961	

Value of up to -20 kJ mol^{-1} is consistent with the electrostatic interaction between the charged molecules and the charged metal (physical sorption), while values more negative than -40 kJ mol^{-1} involves sharing or transfer of electrons from the inhibitor molecules to the metal surface to form a coordination type of bond (chemisorption) [25]. In the present study, the value of ΔGa is less than -20 kJ mol^{-1} which is an indication that physical adsorption in dominant.

SEM-EDX analysis

Surface morphology of iron was studied by scanning electron microscopy after 1 h immersion in 0.5 M HCl with and without addition of the inhibitor. Figure 11(a) represents the micrograph obtained of polished steel before exposing to the corrosive medium while Fig. 11(b) showed strongly damaged steel surface due to the corrosion effect after immersion in 0.5 M HCl

solution. SEM images of steel surface after 1hour immersion in 0.5 M HCl with 1g/100ml TRE is shown in Fig. 11(c). It can be seen from Fig. 11a that the iron sample before immersion seems smooth and shows some abrading scratches on the surface. Inspection of Fig. 11b reveals that the iron surface after immersion in uninhibited 0.5 M HCl shows an aggressive attack of the corroding medium on the iron surface. In contrast, in the presence of 1g/100ml TRE (Fig. 11c) the iron surface was corroded only negligibly. In addition, there was an adsorbed film on the iron surface that was not observed in Fig. 11b. These results confirmed enhancement of surface coverage of steel surface that led to decrease in contact between the iron and the aggressive medium. Thus, a good adsorptive protection layer that was formed by the inhibitor can efficiently inhibit corrosion of steel.
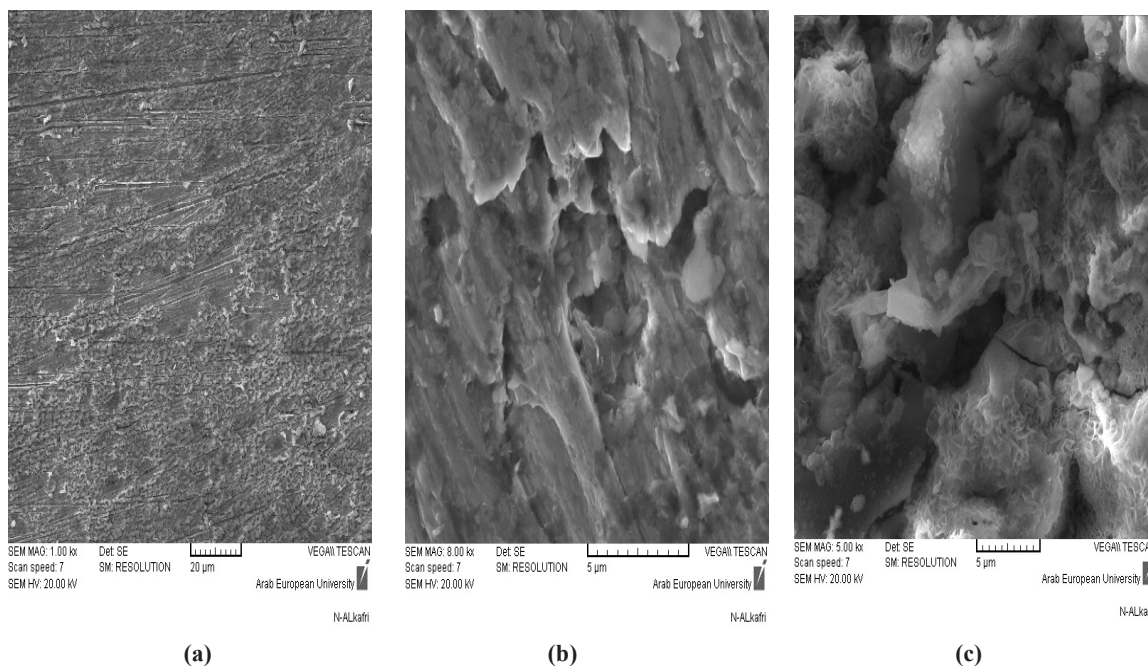
(a)

(b)

(c)

Fig. 11. SEM of polished iron (a) before immersion (b) after 1hour of immersion in 0.5M HCl 1g/100ml of TRE, and (c) Treated iron in the presence of 1g/100ml extract.

The following table shows the percentages of the studied elements in the presence and absence of TRE.

TABLE 6. The percentages of the studied elements in the presence of TRE.

Element	C	O	Cl
Without inhibitor	0.20	-----	-----
After adding 0.5 M HCl	0.20	29.86	1.76
With inhibitor	26.84	7.14	0.1

The iron surface is analyzed at different points of the surface using an energy dispersive x-rays technique. Since the inhibitor contains mainly carbon and oxygen atoms, and the corrosive media is 0, 5 HCl, the variation of carbon, oxygen and chlorine atoms weight percentage on the surface can be used quantitatively to explain the adsorption of the inhibitor on the iron surface. In the presence of the extract the weight percentage (wt. %) of carbon increased while chlorine decreased, as that the atom of oxygen is higher in the presence of the corrosive media composed to the polished and treated iron, as shown in Fig. 12. Thus it can be concluded that there is a good protective layer on the surface of iron is responsible for inhibition.

Conclusion

The following results can be mentioned briefly:
1- The inhibition efficiency (IE%) of TRE increases with increase of extract concentration.
2- EIS results showed that the double layer capacitance (C_{dl}) decreases and charge transfer resistance (R_{ct}) increases with time of immersion in the extract.
3- The inhibitor showed maximum inhibition efficiency (IE%) 88.9% at 8g/100ml concentration.
4- The inhibition efficiency (IE%) of TRE decreased with temperature, which leads to a decrease in activation energy (Ea) of the corrosion process.
5- The activation energy value of Ea= -20kJmol^{-1} indicates that the adsorption process is spontaneous and is physical adsorption.
6- Langmuir adsorption isotherm and SEM studies showed that TRE inhibitions occur through adsorption mechanism.
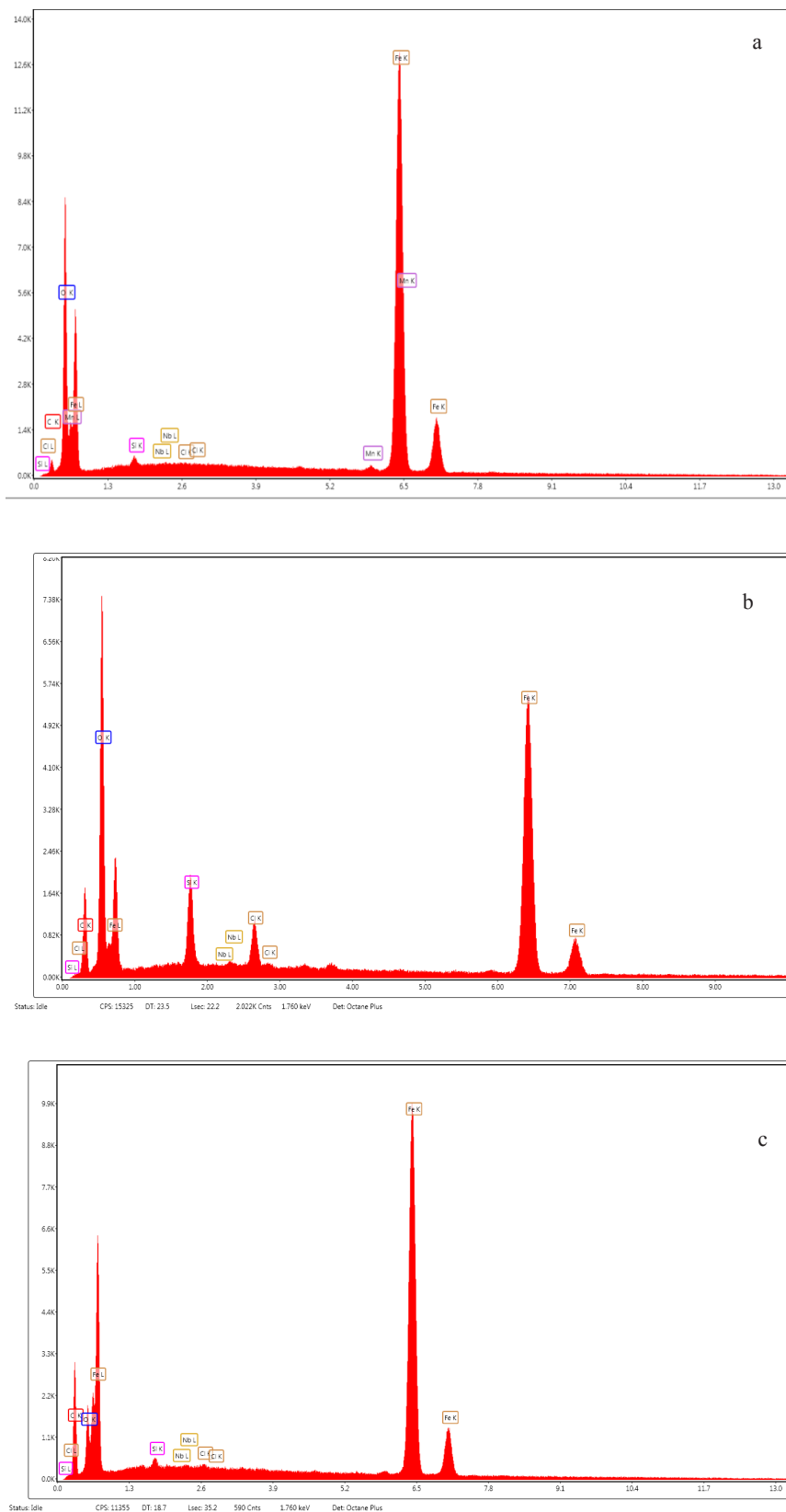7- The results of SEM and EDX, have been shown to form a protective film on the iron surface.

Fig. 12. EDX of (a) polished iron ; (b) after 1hour of immersion in 0.5M HCl, and (c) Treated iron in the presence of 1g/100ml extract.

Acknowledgment

References

1. Ahmed A., Amir H. Kadhum and Abdulhadi K., Inhibition of mild steel corrosion in sulfuric acid solution by new Schiff base. *Process Engineering, University Kebangsaan Malaysia.*, **7**, 787-804 (2014).

2. Ferreira, E.S., Giacomelli, C., Giconelli, F.C. and Spinelli, A., Evaluation of the inhibitor effect of L-Ascorbic acid on the corrosion of mild steel. *Materials Chemistry and Physics*, **83**, 129-134 (2004).

3. Bentiss, F. Gassama, D. Barbry, L. Gengembre, H. Vezin, M. Lagrene´e, Traisnel M., Corrosion inhibition of mild steel in acidic media using newly synthesized heterocyclic organic molecules: Correlation between inhibition efficiency and chemical structure. *Appl. Surf. Sci.* **252** (2006).

4. Lagrenee, M, B. Mernari, N. Chaibi, M. Traisnel, H. Vezin and Bentiss F., Corrosion inhibition of mild steel in acidic media using newly synthesized heterocyclic organic molecules: Correlation between inhibition efficiency and chemical structure. *Corros. Sci.* **43** (2001).

5. Ayers, R.C., Jr. Hackerman, N., Corrosion inhibition in HCl using methyl pyridines. *J. Electrochem. Soc.,* **110** (6), 507-513 (1963).

6. Moretti, G., Guidi, F. and Grion, G., Tryptamine as a green iron corrosion inhibitor in 0.5M deaerated sulphuric acid. *Corrosion Sci.,* **46** (2), 387- 403 (2004).

7. Quraishi, M. A., Rawat, J. and Ajamal, M., Dithiobiurets: A novel class of acid corrosion inhibitors for mild steel. *J. Appl. Electrochem.,* **30** (6), 745- 751 (2000).

8. Khalil, N., Quantum Chemical Approach of Corrosion Inhibition. *Electrochimica Acta,* **48**, 2635- 2640 (2003).

9. Johnsirani, V. J. Sathiyabama, S. Rajendran and Nagalakshmi R., Curcumin dye as corrosion inhibitor for carbon steel in sea water. *Chem. Sci. Trans.* 744–753 (2013).

10. Abdel-Gaber, Khadija M. Hijazia, Ghassan O. Younesa and Bilal Nsouli., Comparative study of the inhibitive action between the bitter orange leaf extract and its chemical constituent linalool on the mild steel corrosion in HCL solution. 230 (2017).

11. Mohamed, H.A., Farag, A.A. and Badran, B.M. Corrosion Inhibition of Mild Steel Using Emulsified Thiazole Adduct in Different Binder Systems. Department of Polymers and Pigments, National Research Center, Cairo, Egypt, 10, 67-77 (2008).

12. Abdel Hamid, Z., Clarification of the corrosion inhibition of mild steel in hydrochloric acid solutions via cetyltrimethyl ammonium bromide inhibitor. Helwan and Department of Chemistry, Faculty of Science, Benha University, Benha, *Egypt J. Chem.* **57** (5,6), 353-371 (2014).

13. Shukla, S. K., Quraishi M. A., The effects of pharmaceutically active compound doxycycline on the corrosion of mild steel in hydrochloric acid solution (HCl). *Corros. Sci.* **52**, 314 (2010).

14. Benali O. L. Larabi, M. Traisnel, L. Gengembra, Y. Harek, Study on the inhibition of mild steel corrosion by quaternary ammonium compound in H_2SO_4 medium. *Appl. Surf. Sci.* **253**, 6130 (2007).

15. Yurt, A. Balaban, S. Ustun Kandemir, G. Bereket, B. Erk, adsorption and corrosion inhibition characteristics of some nicotinamide derivatives on mild steel in hydrochloric acid solution (HCl). *Mater. Chem. Phys.* **85** (2004).

16. Abd EI-Rehim, S, M. A. M. Ibrahim, K. F. Khaled, J., 4-Aminoantipyrine as an inhibitor of mild steel corrosion in HCl solution. *Appl. Electrochem.* **29** (1999).

17. Wen-Ming Ch, Post F, Joshua L, Suresh., Sazzadur R, and Anjali T., Sub-surface Corrosion Research on Rock Bolt System, *Perforated SS Sheets and Steel Sets for the Yucca Mountain Repository.* **30** (2004).

18. Bentiss,F, M. Bouanis, B. Mernari, M. Traisnel, H. Vezin, M. Lagrenee, *Appl. Surf. Sci.* **253** (2007).

19. Ehteram A. Noor, Aisha H. Al-Moubaraki Thermodynamic study of metal corrosion and inhibitor adsorption processes in mild steel/1-methyl-4[4_(-X)-styryl pyridinium iodides/hydrochloric acid systems, *Mater. Chem. Phys.* 110, 145- 154 (2008).

20. Sayyah, S.M., Abd El-Rehim, M.M., Mohamed S.M., Corrosion inhibition of aluminium with a series of aniline monomeric surfactant and their analogues polymers in 0.5 M HCl solution. Chemistry Department, Faculty of Science, Ain Shams University, Cairo, *Egypt J. Chem.* **55** (6), 583– 602 (2012).

21. Maqsood A., M., Ali H., Firdosa N., Shaeel Ah, Zaheer Kh., Anti-corrosion ability of surfactants. *Int. J. Electrochem. Sci.*, **6,** 1927 - 1948 (2011).

22. Abd El-Rahim, S. S., M Refaey, S. A., Taha,

F. B., Saleh, M., Ahmed, R. A., Novel cationic surfactants from fatty acids and their corrosion inhibition efficiency for carbon steel pipelines in 1 M HCl. *J. Appl. Electrochem.* **31** (2001).

23. Abd El-Rehim, S. S., Hassan, H. H., Amin, M. A. Corrosion inhibition of aluminum in hydrochloric acid solution (HCl) using potassium iodate inhibitor. *Mater. Chem. Phys.* **70** (2001).

24. Bilgic, S., Caliskan N., Inhibition of steel corrosion

in hydrochloric acid solution (HCl) by chamomile extract. *Appl. Surf. Sci* **152** (1999).

25. Tsuru, T. Haruyama, S. Gijutsu, B., Corrosion monitor based on impedance method; construction and its application to homogeneous corrosion, *Jpn. J. Soc. Corros. Eng* **27** (1978).

مطيافية المعاوقة الكهروكيميائية (EIS) ودراسة تثبيط تأكل الحديد باستخدام جذور الكركم (TRE) في محلول حمض كلور الماء

خلود المزرزع، أحمد فلاح، أيمن المصري و حسن كلاوي

قسم الكيمياء ـ كلية العلوم – جامعة دمشق ـ سوريا.

دُرس تأثير مستخلص جذور نبات الكركم (TRE) في تثبيط تأكّل الحديد في وسط من حمض كلور الماء (٠،٥ HCl) بالاستقطاب البوتانسيومتري ومطيافية المعاوقة الكهركيميائية (EIS)، أظهرت نتائج نيوكست ازدياد مقاومة انتقال الشحنة (Rct) والمقاومة الاستقطابية (Rp) وتناقص سعة الطبقة المضاعفة (Cdl) بزيادة مدة الغمس في المستخلص. تزداد قيمة كفاءة التثبيط يازدياد حجم المثبط بلغت أفضل قيمة لها ٨٨,٩٠ ٪ عند حجم ٨غ\١٠٠مل، كما دلت قيمة طاقة التنشيط أن امتزاز المثبط المدروس هو من النوع الفيزيائي. وعززت الدراسة السطحية تشكل الفلم المثبط وقيامه بالتثبيط باستخدام مجهر الماسح الالكتروني(SEM) وطاقة تشتت اشعة X (EDX).